BUILD SIMUL (2021) 14: 617–631
https://doi.org/10.1007/s12273-020-0678-2

Research Article

Experimental investigation of evaporative cooling systems for agricultural storage and livestock air-conditioning in Pakistan

Hafiz M.U. Raza[1,2], Muhammad Sultan[1,2] (✉), Majid Bahrami[2], Alamgir A. Khan[3]

1. Department of Agricultural Engineering, Bahauddin Zakariya University, Bosan Road, Multan 60800, Pakistan
2. Laboratory for Alternative Energy Conversion (LAEC), School of Mechatronic Systems Engineering, Simon Fraser University, Surrey, BC, Canada
3. Department of Agricultural Engineering, Muhammad Nawaz Shareef University of Agriculture, Multan 60000, Pakistan

Abstract

Evaporative cooling (EC) is an ancient technique that is usually suitable for hot and dry climatic conditions due to the potential of water vapor evaporation. In this study, three kinds of evaporative cooling systems such as direct EC (DEC), indirect EC (IEC), and Maisotsenko cycle EC (MEC) were locally developed at lab-scale. The performance of the systems was evaluated and compared for agricultural storage and livestock air-conditioning application in Pakistan. The experiments were performed for climatic conditions of Multan city (Pakistan) and the data were collected for hourly and daily basis. According to the results, it was observed that the DEC system has the ability to reduce the temperature of ambient air to an average of 8.5 °C. Whilst IEC and MEC systems were able to drop the temperature of ambient air to an average of 6.8 °C and 8.9 °C, respectively. As per the results, the DEC system remained behind to provide desired conditions for livestock and agricultural product storage applications due to excessive humidity. On the other hand, the IEC and MEC systems can achieve the desired conditions for livestock application, but could not provide feasible conditions for various fruits and vegetable storage. The study concludes that hybrid EC systems can be developed to provide desired conditions for a wide range of applications under varying climatic conditions.

Keywords

evaporative cooling,
air-conditioning,
dew-point,
wet-bulb,
storage,
livestock

Article History

Received: 15 January 2020
Revised: 15 June 2020
Accepted: 17 June 2020

Building Systems and Components

1 Introduction

Temperature and humidity control are necessary for thermal comfort and industrial applications (Tariku et al. 2011; Sultan et al. 2018; Mahmood et al. 2019). Only in the case of buildings, the air-conditioning (AC) systems consume nearly 48% of the entire building energy of the world (Zhuang et al. 2020). This demand will increase with the increase in world's population that is expected to increase by 2 billion in the next 30 years i.e. nearly 9.7 billion persons in total in 2050 (Chen et al. 2020; Li et al. 2020). It is worth mentioning that air-conditioning is not only necessary for humans but also for various applications including (but not limited to) fruits and vegetable storage, livestock thermal comfort etc. (Sultan and Miyazaki 2017; Mahmood et al. 2019). Pakistan has an agriculture-based economy and nearly produces 12 million tons of fruits and vegetables each year. Approximately 35% of these agricultural products are perished away due to post-harvest losses (Sultan and Miyazaki 2017; Mahmood et al. 2020b). In the 21st century, optimal storage and handling of agricultural products are vital for biosafety standards in the global market due to the involvement of biological and physiochemical processes (Sultan and Miyazaki 2017; Mahmood et al. 2020a). Similarly, different animals have various AC requirements depending on multiple parameters including metabolism rate, respiration rate, skin heat transfer, genetic factor and nature of the feed etc. (Rose et al. 1996; Karimi et al. 2015; Niaz et al. 2019). The airflow/ventilation rate is an important factor for animal AC. Different techniques are used for storage purposes. In this regard, American Society of Heating, Refrigeration, and Air-Conditioning Engineers (ASHRAE) recommends the range values of humidity and temperature for ideal thermal comfort of animals (ASHRAE 2007, 2009). The ideal storage for generalized

E-mail: muhammadsultan@bzu.edu.pk; muhammad_sultan@sfu.ca

List of symbols

A	area [m^2]	Q_i	infiltration load [kW]
AC	air-conditioning	Q_l	lamps heat load [Wh/day]
ASHRAE	American Society of Heating, Refrigeration, and Air-Conditioning Engineers	Q_p	personal load [kW]
		Q_r	heat of respiration [kW]
C	convection heat loss from respiration [W/(h·m^2)]	Q_t	transmission load [kW]
C_p	specific heat capacity of air [J/(kg·K)]	r	respiration heat [kJ/(kg·day)]
DEC	direct evaporative cooling	RH	relative humidity [%]
E	evaporation heat loss from respiration [W/(h·m^2)]	S	heat stored in the body [kW]
EC	evaporative cooling	t	time [h]
h	enthalpy [kJ/kg DA]	T	temperature [°C or K]
H	heat loss [W/h]	T_a	ambient air temperature [°C or K]
IEC	indirect evaporative cooling	T_{db}	dry bulb temperature [°C or K]
m	mass [kg]	T_{dp}	dew point temperature [°C or K]
M	metabolic rate [met]	T_{in}	inlet temperature [°C or K]
M-cycle	Maisotsenko cycle	T_{out}	outlet temperature [°C or K]
MEC	M-cycle evaporative cooling	T_{wb}	wet bulb temperature [°C or K]
n	number of air changes [—]	U	overall heat transfer coefficient [W/(m^2·K)]
N_f	number of fans [—]	v	velocity [m/s]
N_l	number of lumps [—]	V	air volume [m^3]
N_p	number of people working in storage chamber [—]	VCAC	vapor compression air-conditioning
p	atmospheric pressure [kPa]	w	humidity ratio [g/kg DA], i.e. [g of water vapor per kg of dry air]
p_a	vapor pressure [kPa]		
P	power [W]	W	weight [kg]
q	partial heat for different parts and objects [kW]	ε_{dp}	dew point effectiveness [—]
Q_a	total heat for animals [kW]	ε_{wb}	wet bulb effectiveness [—]
Q_e	equipment load [kW]	ρ	density of air [kg/m^3]
Q_f	fan heat load [Wh/day]	σ	uncertainty in effectiveness [—]

agricultural products and thermal comfort zones for livestock are shown in Figure 1 (Mahmood et al. 2019; Niaz et al. 2019).

Various types of AC options/techniques are explored worldwide in order to obtain desired temperature and humidity conditions for thermal comfort as well as for associated applications. Sghiouri et al. (2020) provided a passive cooling technique comparison in reducing overheating of clay-straw building. Ameur et al. (2020) optimized the passive design features for a naturally ventilated residential building. Typically, two kinds of AC systems are used in Pakistan i.e. (i) swamp air cooler (DEC) which is a low-cost solution, and (ii) vapor-compression AC (VCAC) system which is a costly option. The performance of the DEC system is low in high humid climatic conditions (Laknizi et al. 2019; Al-Zubaydi and Hong 2019), while VCAC systems cause the emission of environmentally harmful refrigerants (Mahmood et al. 2016; Dizaji et al. 2018; Dai and Sumathy 2002). These gases are also responsible for ozone layer depletion and global warming (Vakiloroaya et al. 2014; Wan et al. 2018; Cihan et al. 2020; Al Horr et al. 2020). The VCAC system also requires high electric power (Khalid et al. 2016; Mahmood et al. 2016; Arun et al. 2020) that is generated mostly from burning of fossil fuels and contribute in the phenomenon of climate change. In Pakistan and other developing countries, research on livestock and agricultural product storage remains neglected due to the high cost involved in the development and maintenance of conventional AC technologies (Sultan et al. 2018).

The available literature depicts the liability of evaporative cooling (EC) systems as a viable alternative to the VCAC system for various applications (Riangvilaikul and Kumar 2010). The EC systems generate cooling by evaporation of water vapors into the air (Camargo et al. 2005; Yuan and Chen 2012; Jeong et al. 2018; Dong and Jeong 2020). These systems usually possess simple design and construction, therefore, considered as low-cost, energy-efficient and environment friendly solution (Senthilkumar and Srinivasan 2012; Zhang et al. 2019; Sibanda and Workneh 2020). Evaporation is caused by the contact of hot air with water

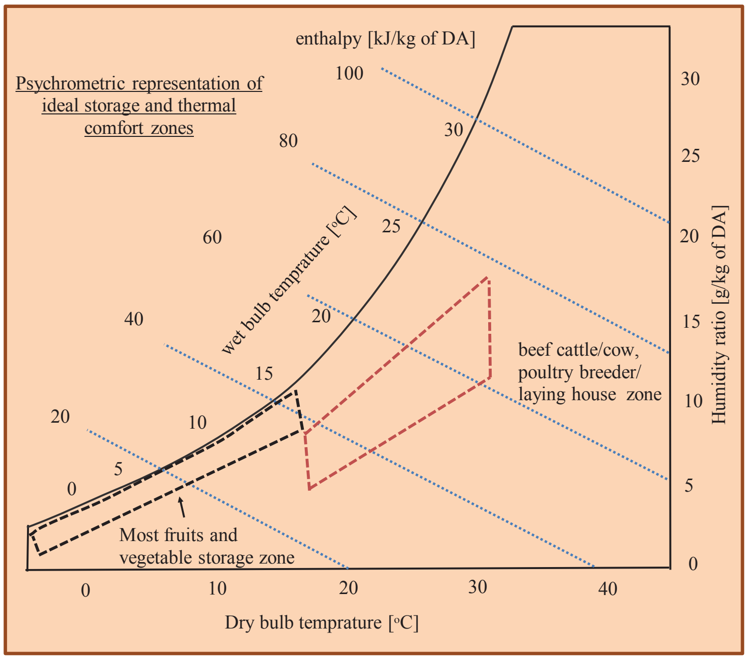

Fig. 1 Ideal storage zone for generalizing agricultural products and thermal comfort zone for livestock

and is energy efficient in the climatic conditions where ambient air is hot and dry and limited at RH_{DEC} and RH_{IEC} > 75%, $w_{MEC} \leq 11.2$ g/kg DA) (Mohapatra and Sanjay 2013; Mahmood et al. 2016; Wan et al. 2018; Nayak et al. 2020). The EC systems consume one-fourth of electricity as compared to the conventional AC systems (Khalid et al. 2016). Besides their multiple benefits, the variety of EC systems is available in developing countries only at limited scale.

This study focusses on the climatic conditions of Multan city which is one of the largest cities of Pakistan with population of more than two million. The city has an arid climate with extremely hot conditions in summer and relatively cold conditions in winter. Its winter season starts from December and ends till February. Heavy rains occur in this season which cause of the decrease in temperature. The spring season starts from March and ends till April where flowers shows are held across the city. The summer season (including monsoon rain season) starts from May and ends till September. The autumn season starts from October and ends till November where dry and hazy weather is the main features of this season. It has humid climatic conditions in the monsoon season (July to September). So, there is a need to control these environmental conditions for different applications regarding the thermal comfort of predetermined space.

As such this study aims to develop lab-scale EC systems with locally available materials. The development includes direct EC (DEC), indirect EC (IEC), and Maisotsenko cycle EC (MEC) systems. The comparative performance evaluation is an important segment of this study. The present study focuses on the feasibility of EC systems for the climatic conditions of Multan (Pakistan), and cost analysis of these systems with 1ton ideal VCAC system.

2 Evaporative cooling (EC) technologies

The EC refers to techniques in which process air is cooled by latent heat variation caused by water vapor evaporating into the air. The study focus three EC systems named as (i) direct EC (DEC), (ii) indirect EC (IEC), and (iii) Maisotsenko cycle EC (MEC) systems. Table 1 provides the detail fundamentals, thermodynamic concepts, schematics and psychrometric representation of the EC systems (Duan et al. 2012; Rafique et al. 2015). The DEC and IEC can cool the air up to the wet-bulb temperature whereas, the MEC can cool up to the dew-point temperature. Therefore, the performance of DEC and IEC is measured in wet-bulb effectiveness, whereas, it is measured in dew-bulb effectiveness in the case of MEC.

The DEC system is the simplest and old technique in which the process air is directly in contact with water vapors (Xuan et al. 2012). In this process, water vapors are evaporated into the air which reduces the process air temperature, however, increases the process air humidity ratio. Ideally, this is an isenthalpic cooling process in which enthalpy of the process air remains the same (Mahmood et al. 2019). The cooling limit of DEC is wet-bulb temperature of process air (at 100% relative humidity). On the other hand, the IEC system can cool the process air up to the wet-bulb temperature while keeping the constant humidity ratio. This

Table 1 Fundamentals of evaporative cooling systems

<table>
<tr>
<td>Evaporative cooling
It refers to techniques in which process air is cooled by latent heat variation caused by water vapor evaporating into the air</td>
<td>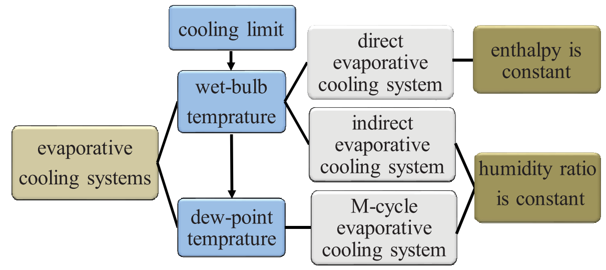
</td>
</tr>
<tr>
<td><u>Direct evaporative cooling (DEC) system</u>
• Air directly contacts with water
• Reduces the temperature and humidifies the air simultaneously
• The thermal process is adiabatic
• Enthalpy of the inlet and outlet air remains the same
$h_{\text{inlet}} = h_{\text{outlet}} = h$ (isenthalpic cooling)
• Humidity ratio of the outlet air is greater than the inlet air
$w_{\text{out}} > w_{\text{inlet}}$
• Wet-bulb effectiveness range of DEC system is 75%–95%</td>
<td><u>DEC</u>
$$\varepsilon_{\text{wb}} = \frac{T_{\text{in}} - T_{\text{out}}}{T_{\text{in}} - T_{\text{wb}}}$$
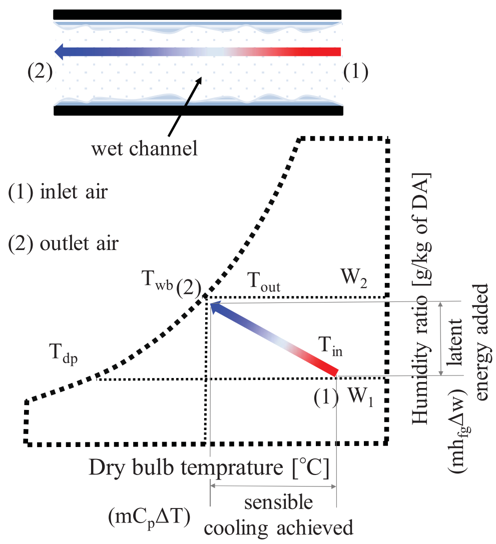
</td>
</tr>
<tr>
<td><u>Indirect evaporative cooling (IEC) system</u>
• Air does not directly contact with water
• It consists of dry and wet channels
• Reduces the air temperature without increasing its moisture
• The cooling effect is produced by two thermodynamic processes: (i) evaporative cooling and (ii) sensible heat transfer
• Humidity ratio of inlet and outlet air remains constant
$w_{\text{out}} = w_{\text{inlet}}$
• Enthalpy of outlet air is less than inlet air
$h_{\text{outlet}} < h_{\text{inlet}}$
• Wet-bulb effectiveness range of IEC system is 50%–65%</td>
<td><u>IEC</u>
$$\varepsilon_{\text{wb}} = \frac{T_{\text{in}} - T_{\text{out}}}{T_{\text{in}} - T_{\text{wb}}}$$
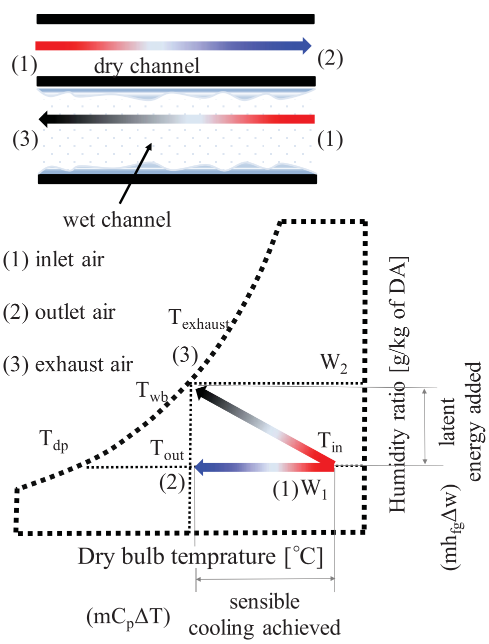
</td>
</tr>
</table>

Table 1 Fundamentals of evaporative cooling systems (Continued)

• Maisotsenko-cycle evaporative cooling (MEC) system • An advanced form of IEC system • The cooling effect is produced by two thermodynamic processes: (i) evaporative cooling and (ii) and sensible heat transfer • Reduces the air temperature closer to its dew-point temperature • Humidity ratio of inlet and outlet air remains the same $w_{\text{out}} = w_{\text{inlet}}$ • Enthalpy of outlet air is less than inlet air $h_{\text{outlet}} < h_{\text{inlet}}$ • Dew-point effectiveness range of the MEC system is 50%–65%	<u>**MEC**</u> $\varepsilon_{\text{dp}} = \frac{T_{\text{in}} - T_{\text{out}}}{T_{\text{in}} - T_{\text{dp}}}$ 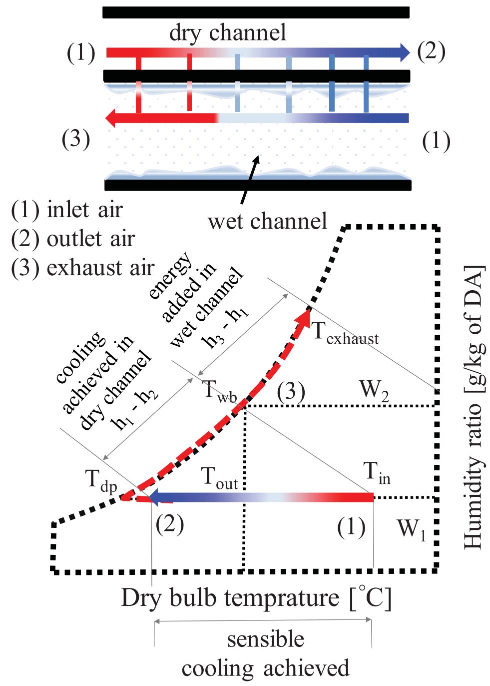

process is realized by adjacent placement of dry and wet channels in such a way that only heat transfer is possible between the channels (Yuan et al. 2020; Matsui et al. 2020). The ambient air is cooled in wet channels (working air) similar to DEC process whereas, the obtained cooling effect is transferred to dry channels (process air) at constant humidity ratio. In addition, EC by means of Maisotsenko cycle (MEC) is an advance form of IEC by which process air can be cooled to dew-bulb temperature (Arun et al. 2020; Lin et al. 2020). In this process, attributes of wet and dry channels are organized in such a way that the resultant cooling effect is accumulated in the product channel which cools the process air up to the dew-point temperature. The process of all three systems is explained in detail in Table 1, whereas, following works can be referred for more insights (Mahmood et al. 2016; Sultan and Miyazaki 2017; Sultan et al. 2018; Niaz et al. 2019; Mahmood et al. 2016, 2019, 2020a,b).

3 Materials and methods

3.1 Experimental apparatus and procedure

3.1.1 DEC unit

A lab-scale experimental setup is developed which consists of a fan (for moving the air), a regulator, a water pump, a storage tank, and evaporative cooling pads. A schematic diagram of the DEC experimental setup is shown in Figure 2. In literature, different types of cooling pads are used as a cooling media which are made up of date palm fiber, cellulose fiber, jute, cotton fiber, etc. (Vala et al. 2014). The DEC system market in Pakistan uses biodegradable cooling pads which are easily available with local name as khus. The efficiency of DEC system is decreased by increasing thickness of the pad due to air pressure drop. Recently, cellulose pads are readily available in the market. These are light in weight and can be constructed into desired shapes (Warke and

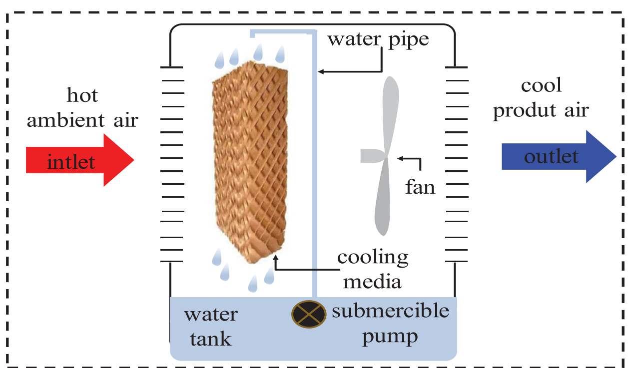

Fig. 2 Schematic diagram of DEC experimental setup

Deshmukh 2017). In this study, Cellulose Fiber 5090 is used as a cooling media which has 70%–95% effectiveness (Amer et al. 2015). The first two numbers of the fiber show the distance between the two head-to-head layers in millimeter and the last two numbers denote the angle between two consecutive corrugated layers. During the experiment, water moves downwards due to gravity and entered in a storage tank where it is recirculated using a low-pressure water pump. In the system, air passes from the cooling pads and is cooled due to a difference in water vapor pressure in the media and air. The detailed parameters of the DEC experimental setup are shown in Table 2.

3.1.2 IEC unit

The developed experimental apparatus for IEC system is presented in Figure 3. The system comprises of 30 aluminum sheets upon which felt (fibrous material) are pasted on one side of the sheets with an adhesive material. The felt is used to hold the thin water film and form a wet channel as it can retain and adsorb water 280 g/m^2 (Zhan et al. 2011). Rubber cord of 4 mm thickness are used as channel guides and placed horizontally and vertically for the dry and wet channels,

Table 2 Design parameters of the DEC system

Design parameters	Values/quantities	Units
Fan type	15 (axial fan)	W
Pump type	10 (submersible pump)	W
Evaporative cooling pad material	Cellulose fiber	—
Length of cooling pad	0.34	m
Width of cooling pad	0.25	m
The thickness of the cooling pad	50.8	mm

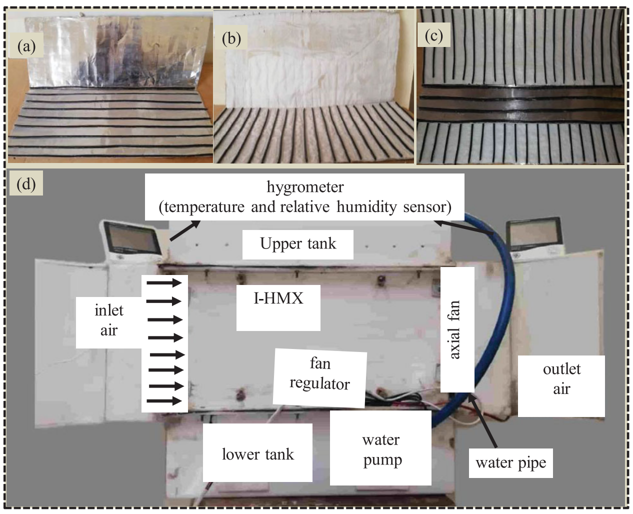

Fig. 3 Pictorial diagram of IEC apparatus: (a) dry channels, (b) wet channels, (c) arrangement of dry and wet channels, (d) IEC apparatus

respectively. Dry to wet channel heat transfer depends on the thickness of aluminum-coated felt sheets, coefficient of convective heat transfer (a function of channel size and airflow rate) and thermal conductivity of the material used (Khalid et al. 2016). Literature suggests a 0.5 mm gap between dry and wet channels, 25 mm spacing between guides of the dry and wet channels (Khalid et al. 2016). Channel guides move horizontally along the width to make wet channels and vertically along the height to make dry channels. Each sheet consists of eight dry channels in the case of a dry side or 20 wet channels for the wet side. The length of the wet channel is 0.20 m and the dry channel is 0.50 m. The experimental system consists of upper and lower water tanks, water pumps, and fan at the outlet. Water moves vertically in wet channels and product air moves horizontally in dry channels, to make crossflow. The detailed design parameters of the IEC experimental setup are given in Table 3.

3.1.3 MEC unit

The developed MEC experimental setup is shown in Figure 4. The system consists of 33 aluminum sheets pasted with felt material. Dimensions of all sheets are the same as those of the IEC system with different design. In dry channels, precise holes with a diameter of 4mm are made for the flow of air from dry to wet channels. Each sheet consists of 8 dry channels and 20 wet channels. In dry channels, the upper 5 channels serve as product channels and the last three channels serve as working channels. In working channels, holes of 4mm diameter are made with the gap of 1 channel. A portion of the working air passed through these holes to reduce the temperature of the ambient air up to the dew-point temperature. The detailed design parameters of the MEC experimental setup are given in Table 3.

Table 3 Design parameters of IEC and MEC systems

Design parameters	Values/quantities	Units
Wall materials	Aluminum sheet pasted with felt	—
Wall thickness	0.5	mm
Length of channel	0.50	m
Width of wet channel	0.20	m
Channel gap	25	mm
Fan type	15 (axial fan)	W
Pump type	10 (submersible pump)	W
Sensors	Hygrometer, anemometer	—
Water absorbing ability to felt	280	g/m^2
Felt conductivity	0.4	W/(m·K)
Outer surface constructed material	5 (plastic sheets)	mm
Joint material	Silicon	—

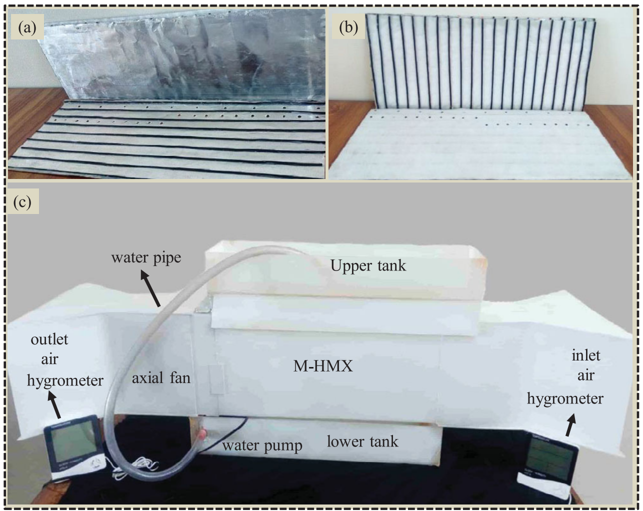

Fig. 4 Pictorial diagram of MEC apparatus: (a) dry channels, (b) wet channels, (c) MEC apparatus

3.2 Cooling load measurements

Cooling system is designed based on peak load required for agricultural product storage and livestock applications. Design schematic diagram and heat transfer phenomenon for animals and agricultural products storage are shown in Figure 5.

3.2.1 Agricultural product storage

In this study, the cooling load is considered for the storage of 3.3 tons (3300 kg) of mangoes. It is worth mentioning that the air temperature of 15 °C and relative humidity ranging from 85% to 95% (with an average of 90%) is required for optimum storage of mangoes. Respiration rate of mangoes is taken as 33.26 kJ/(kg·day) (Ravindra and Goswami 2008; Mohapatra et al. 2013; Raza et al. 2013; Patel et al. 2016). The dimensions of storage room are considered as 3.6 m length, 3.6 m width and 3.6 m height. It is important to mention that the cooling load comprises of transmission load (Q_t), heat of respiration (Q_r), personnel load (Q_p), equipment load (Q_e) and air infiltration load (Q_i) and measure as follows:

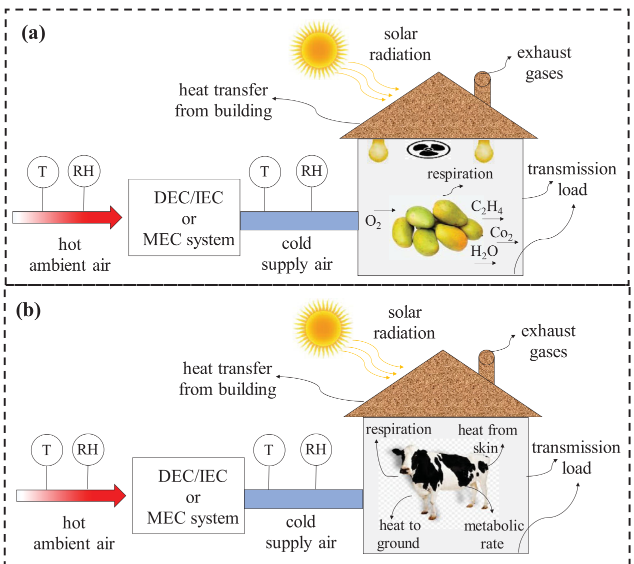

Fig. 5 Design schematic diagram and heat transfer phenomenon for: (a) mango storage, and (b) cow cattle farm

$$Q_t = UA(T_{out} - T_{in}) \tag{1}$$

where, Q_t is in [kW]. The U is the overall building heat transfer coefficient [W/(m^2·K)], and A is the building area [m^2]. T_{out} is the ambient air temperature outside the storage area [°C], and T_{in} is the temperature inside the storage area [°C]. After harvesting, agricultural products behave like as living organism and respire as given by Eq. (2) (Mahmood et al. 2020b). Oxygen presented in ambient air reacts with sugar of product to produce carbon dioxide, water, and respiration heat.

$$C_6H_{12}O_6 + 6O_2 \rightarrow 6CO_2 + 6H_2O + \text{respiration heat} \tag{2}$$

The heat of respiration (Q_r) is given by following relationship:

$$Q_r = mr \tag{3}$$

where, Q_r is in [kW] and r is the daily respiration heat [kJ/(kg·day)]. The personnel heat load (Q_p) is given by the following relationship:

$$Q_p = N_p Ht \tag{4}$$

where, Q_p is in [kW]. The N_p is the number of people working inside per day, t is the working hours [h] and H is the heat loss per person [W/h]. The equipment load (Q_e), the fan heat load (Q_f), and the lamps heat load (Q_l) are estimated as follows:

$$Q_e = Q_f + Q_l \tag{5a}$$

$$Q_f = N_f Pt \tag{5b}$$

$$Q_l = N_l HPt \tag{5c}$$

where Q_e is in [kW], Q_f is in [Wh/day], and Q_l is in [Wh/day]. The N_f is the number of fans, N_l is the number of lamps, t is the time used per day (h) and the power (P) is the wattage of equipment [W]. The air infiltration load (Q_i) is given by following relationship:

$$Q_i = nV\rho C_p (T_{out} - T_{in}) \tag{6}$$

where, n is the air changes per day, V is the air volume [m^3], C_p is the specific heat of air [kJ/(kg·K)] and ρ is the air density [kg/m^3].

3.2.2 Livestock thermal comfort

For livestock application, the cooling load is calculated for cattle farm of 50 Holstein Friesian cows. The dimensions of cattle farm are taken as 150 m length, 50 m width and 9 m height. The cooling load requirement is calculated for ideal thermal comfort of Holstein Friesian cows in cattle farm. The average weight of cow is presumed 560 kg. The cooling load is calculated by using set of Eqs. (7) to (9) (ASHRAE 2009; Wang et al. 2018; Sultan et al. 2019).

$$Q_{\mathrm{a}} = q_{\mathrm{respiratory}} + q_{\mathrm{skin}} + S \tag{7}$$

where, Q_{a} is the total heat for animals [kW]. The q is the partial heat for different parts and objects [kW]. The S represents the heat stored in the body and for ideal heat balance ($S = 0$). The numerical value of $q_{\mathrm{respiratory}}$ per unit hour and per unit m^2 is determined using Eq. (8a):

$$q_{\mathrm{respiratory}} = E_{\mathrm{respiratory}} + C_{\mathrm{respiratory}} \tag{8a}$$

$$E_{\mathrm{respiratory}} = 0.0173M(5.87 - p_{\mathrm{a}}) \tag{8b}$$

$$C_{\mathrm{respiratory}} = 0.0014M(34 - T_{\mathrm{a}}) \tag{8c}$$

where, C represents the convection heat loss from respiration [W/(h·m^2)] and E represents the evaporation heat loss from respiration [W/(h·m^2)]. The M represents the metabolic rate [met] where 1 met is equal to 58.2 W/m^2. The T_{a} and p_{a} represent the ambient air temperature [°C] and the vapor pressure [kPa], respectively.

$$q_{\mathrm{skin}} = MA_{\mathrm{skin}} \tag{9a}$$

$$A_{\mathrm{skin}} = 0.147W^{0.57} \tag{9b}$$

where, A_{skin} is the skin area [m^2] and W is the animal weight [kg].

3.3 Uncertainty analysis

The uncertainty analysis is carried out for the effectiveness of the systems' performance data by using root of sum of squares method as given by Eq. (10) (Mahmood et al. 2020b). Values of individual uncertainties are provided by manufacturer of the sensors i.e. uncertainty in T, RH, and v are ±1 °C, ±5%, and ±1 m/s, respectively. The overall uncertainty of systems' effectiveness is determined as follows:

$$\sigma t = \pm\sqrt{\sigma T^2 + \sigma \mathrm{RH}^2 + \sigma v^2} \tag{10a}$$

$$\sigma\varepsilon_{\mathrm{wb}} = \pm\sqrt{\left(\frac{\delta\varepsilon_{\mathrm{wb}}}{\delta T_{\mathrm{out}}}\sigma T_{\mathrm{out}}\right)^2 + \left(\frac{\delta\varepsilon_{\mathrm{wb}}}{\delta T_{\mathrm{wb}}}\sigma T_{\mathrm{wb}}\right)^2} \tag{10b}$$

$$\sigma\varepsilon_{\mathrm{dp}} = \pm\sqrt{\left(\frac{\delta\varepsilon_{\mathrm{dp}}}{\delta T_{\mathrm{out}}}\sigma T_{\mathrm{out}}\right)^2 + \left(\frac{\delta\varepsilon_{\mathrm{dp}}}{\delta T_{\mathrm{dp}}}\sigma T_{\mathrm{dp}}\right)^2} \tag{10c}$$

where, $\sigma\varepsilon_{\mathrm{wb}}$ and $\sigma\varepsilon_{\mathrm{dp}}$ denote the uncertainty in wet-bulb and dew-point effectiveness of the experimental systems. The σT_{out}, σT_{wb}, and σT_{dp} represent the digital hygrometer thermometer instrument uncertainties i.e. ±1 °C. Uncertainty in the wet bulb effectiveness of DEC, IEC and MEC systems is ±0.08, ±0.09, and ±0.08, respectively. In the case of the MEC system, the uncertainty in the dewpoint effectiveness is ±0.09.

3.4 Data reduction

The psychrometric parameters (temperature, relative humidity, specific humidity, and enthalpy) are estimated by the following equations (Riangvilaikul and Kumar 2010; Stull 2011; Miyazaki et al. 2011; Doğramacı and Aydın 2020; Mahmood et al. 2020b).

$$\begin{aligned} T_{\mathrm{wb}} = {} & T\tan^{-1}\left[0.151977 + (\mathrm{RH} + 8.313659)^{\frac{1}{2}}\right] \\ & + \tan^{-1}(T + \mathrm{RH}) - \tan^{-1}(\mathrm{RH} - 1.676331) \\ & + 0.00391838\mathrm{RH}^{\frac{3}{2}}\tan^{-1}(0.023101\mathrm{RH}) - 4.686035 \end{aligned} \tag{11}$$

$$T_{\mathrm{dp}} = T_{\mathrm{db}} - \frac{100 - \mathrm{RH}}{5} + 0.9 \tag{12}$$

$$h = 1.006T + W(2501 + 1.86T) \tag{13}$$

$$w = 0.62195\left(\frac{P_{\mathrm{w}}}{P - P_{\mathrm{w}}}\right) \tag{14}$$

$$\mathrm{RH} = \frac{P_{\mathrm{w}}}{P_{\mathrm{ws}}} \tag{15}$$

where, T_{db} is the dry-bulb temperature [°C], RH is the relative humidity [%], h is the enthalpy [kJ/kg], P is the pressure [Pa] and w is the humidity ratio [g/kgDA].

The wet-bulb and dew-point effectiveness are calculated by Eqs. (16) and (17), respectively (Bruno 2011; Boonyasri et al. 2017; Jaafarian 2018; Mahmood et al. 2019; Yuan et al. 2020).

$$\varepsilon_{\mathrm{wb}} = \frac{T_{\mathrm{in}} - T_{\mathrm{out}}}{T_{\mathrm{in}} - T_{\mathrm{wb}}} \tag{16}$$

$$\varepsilon_{\mathrm{dp}} = \frac{T_{\mathrm{in}} - T_{\mathrm{out}}}{T_{\mathrm{in}} - T_{\mathrm{dp}}} \tag{17}$$

where, $\varepsilon_{\mathrm{wb}}$ and $\varepsilon_{\mathrm{dp}}$ represent the wet-bulb and dew-point effectiveness, respectively.

4 Results and discussion

The experimental data from the developed EC systems i.e. DEC, IEC, and MEC are obtained for the different climatic conditions of Multan (Pakistan). The monthly (average) temperature and relative humidity of ambient air for climatic conditions of Multan is shown in Figure 6. The climatic conditions data are obtained from the Metronome 7 software. The inlet air velocity is ranging between 4 and 5 m/s in the case of the MEC and IEC system, whereas, it is 2–3 m/s in the case of DEC system. The outlet velocity of air is ranging between 2 and 3 m/s in the case of MEC and IEC, whereas, it is 1–2 m/s in the case of DEC system.

Performance of the systems is evaluated on hourly based data for the day of 16-May and daily based data for April. Hourly based variation in temperature and relative humidity of ambient and product air for the developed systems on May 16 is shown in Figure 7. Solid lines containing solid filled markers show the variation in temperature of ambient air, and product air of DEC, IEC, and MEC systems. However, broken lines containing blank markers are indicators for the variation in relative humidity of ambient air and product air conditions accordingly. It was noticed that DEC, IEC, and MEC temperature lines run below the ambient air temperature line. From H_1 to H_7 (1 a.m. to 7 a.m.) temperature variation trend lines show the decreasing behavior. Moreover, during this period, the temperature of ambient air decreased. As a result of this phenomenon, the trend lines of evaporative cooling systems slide downward. From H_7 to H_{15} (7 a.m. to 2 p.m.) temperature variation trend lines show the increasing behavior. It is noticed that during this time temperature of ambient air was increasing, therefore from H_7 to H_{15} the performance of the systems is high. The peak temperature of ambient air which was observed on 16 May for $H_{15\text{-}16}$ was 35.5 °C. It was observed that the performance of the evaporative cooling systems reached a maximum at a peak temperature of ambient air. The observed temperatures of product air at this point were 25 °C, 27 °C, and 23 °C for DEC, IEC, and MEC systems, respectively. From H_1 to H_7 (2 p.m. to 12 a.m.) temperature variation trend lines show the decreasing behavior. It shows that during this time the temperature of ambient air is decreased. It was cleared that the performance of the systems depends on ambient air conditions. It was observed that, when the temperature of ambient air was decreased, the relative humidity of product air will increase. The minimum relative humidity observed at H_{17} was 37% and at this point, the relative humidity of the product air of the DEC system was 80%, the IEC system was 59%, and the MEC system was 78%. Ambient air temperature for the day of 16-May on hourly basis data was ranging from 26 °C to 35.8 °C. Test results displayed a noticeable cooling effect (i.e. difference of ambient and product air temperatures) was ranging from 6.2 to 9.6 °C in the case of the DEC system. In the case of IEC and MEC systems, the cooling effect was ranging from 3.2 to 6.2 °C and 5.3 to 12.3 °C.

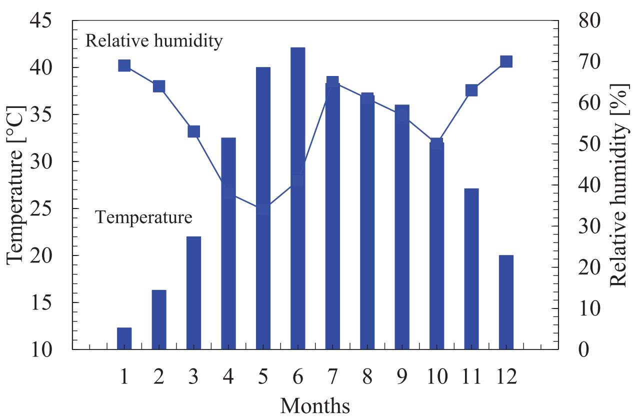

Fig. 6 Monthly (average) temperature and relative humidity of ambient air for climatic conditions of Multan (Pakistan)

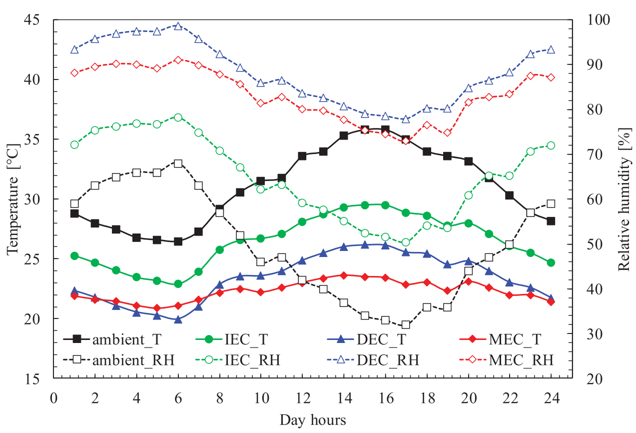

Fig. 7 Variation in temperature and relative humidity of ambient air and product air of the developed systems for 16 May on hourly basis data

Figure 8(left) shows the variation in the humidity ratio of ambient air and product air. The variation of relative humidity is shown with bar lines. In this figure, solid filed bar line shows the variation in humidity ratio of ambient air and pattern filed shows the variation in humidity ratio of product air. It was observed that in the case of MEC and IEC systems the humidity ratio of ambient air and product air is the same but in the case of the DEC system, it is changed. Because the DEC system reduced the temperature of ambient air with the addition of humidity (Wan et al. 2018). But the IEC and MEC systems reduced the temperature without the addition of humidity (Sultan and Miyazaki 2017). Figure 8(right) shows the variation in enthalpy of ambient air and product air. The variation of enthalpy is shown with bar lines. In this figure, a solid filed bar line shows the variation in enthalpy of ambient air and pattern filed shows the variation in enthalpy of product air. It was observed that in the case of the DEC system the enthalpy of ambient air and product air is the same but in the case of the IEC and MEC systems, it is changed. Because the DEC system

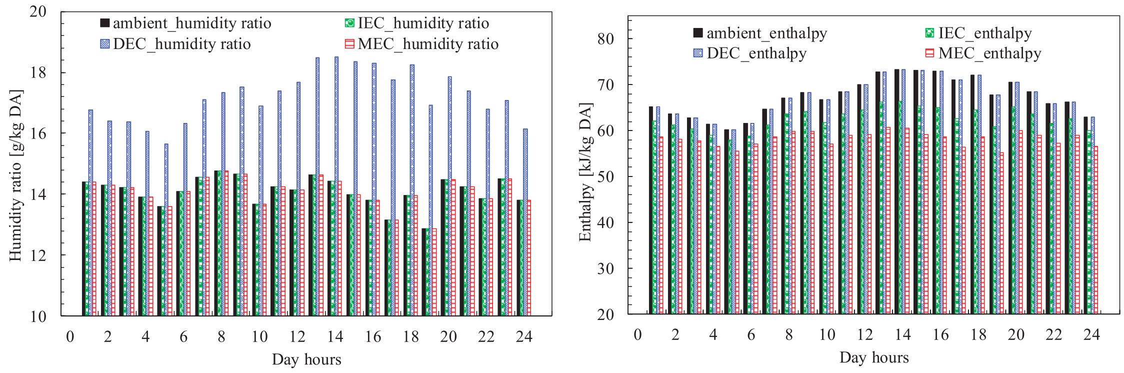

Fig. 8 Thermodynamic properties of ambient air and product air of the developed systems for 16-May on hourly basis data: (left) variation in humidity ratio, and (right) variation in enthalpy

has isenthalpic cooling potential. But IEC and MEC systems provide sensible cooling.

Figure 9 shows variation in temperature and relative humidity of ambient air and product air of the developed systems for April on daily basis data. It is important to mention that the climatic conditions data are obtained from the Metronome 7 to check the performance of developed systems. The peak temperature of ambient air which observed at D_{12} was 35.5 °C. At this temperature, the performance of the evaporative cooling systems was the maximum. The observed temperature of the product air of the DEC system at this point was 22.3 °C. The IEC system at this point was 25.7 °C, and the MEC system at this point was 21 °C. The peak relative humidity of ambient air which observed at D_{12} was 42.8%. At this point, the observed relative humidity of the product air of the DEC system was 64.9%, the IEC system was 55.8%, and the MEC system was 72.9%. Ambient air temperature for April was ranging from 21.5 to 33.9 °C and the range of relative humidity was from 30 to 58%. Sensible cooling effect (i.e. difference of ambient and product air temperatures) of the DEC system was ranging from 6.5

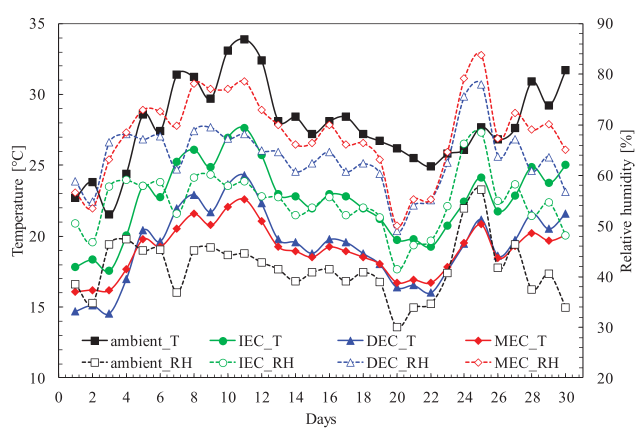

Fig. 9 Variation in Temperature and relative humidity of ambient air and product air of the developed systems for April on daily basis data

to 10 °C. In the case of IEC and MEC systems, the cooling effect was ranging from 3.9 to 6.7 °C and 5.3 to 11.6 °C, respectively.

Thermodynamic properties of ambient air and product air of the developed systems for April are analyzed on daily basis data for (a) variation in humidity ratio, and (b) variation in enthalpy. Figure 10(a) shows the variation in the humidity ratio of ambient air and product air. It was noticed that in the case of MEC and IEC systems the humidity ratio of ambient air and product air is the same but in the case of the DEC system, it is changed. Figure 10(b) shows the variation in enthalpy of ambient air and product air. It was clear that in the case of the DEC system the enthalpy of ambient air and product air was not different but in the case of IEC and MEC systems, it is changed.

Performance of the systems is investigated in terms of wet-bulb and dew-point effectiveness as defined by Eqs. (16) and (17). The results for all the systems are plotted in Figure 11 which also show the experimental error. The detailed uncertainty analysis results (monthly basis) of the wet-bulb effectiveness are given in Table 4 for all the systems. In addition, a comparison of wet-bulb effectiveness is made for the developed EC system on hourly basis variation for 16-May, and on daily basis variation for April as shown in Figure 12. According to variation in hourly basis data for 16-May, the wet-bulb effectiveness of the DEC system ranges from 0.85 to 0.99, for the IEC system its ranges from 0.55 to 0.56 and for the MEC system its ranges from 0.85 to 0.98. According to the variation in daily basis data for April the wet-bulb effectiveness of the DEC system ranges from 0.85 to 0.98, for the IEC system its value ranges from 0.53 to 0.57 and for the MEC system effectiveness ranges from 0.58 to 0.98. In addition, variation in temperature, relative humidity, enthalpy, humidity ratio, and wet-bulb effectiveness of the developed systems for the months of May and June, are provided in the Appendix via Figure A1 to Figure A5, which is available in the Electronic Supplementary Material (ESM) in the online version of this paper.

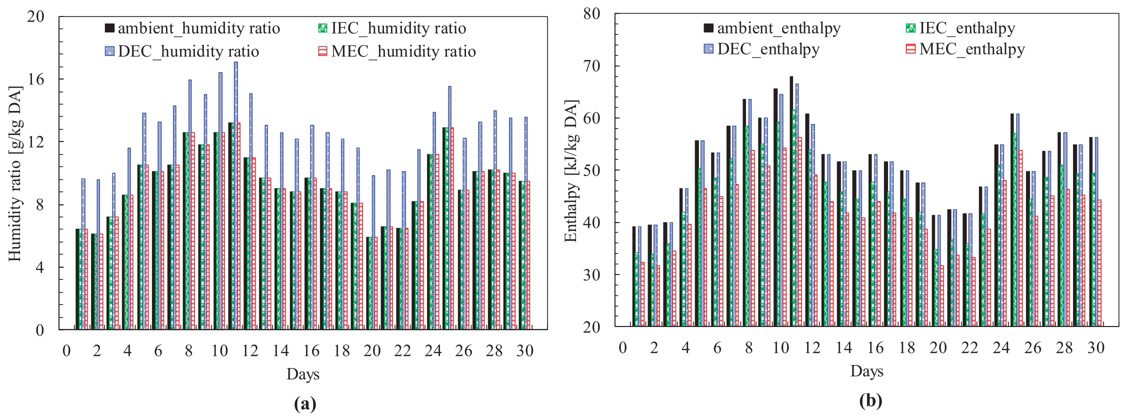

Fig. 10 Thermodynamic properties of ambient air and product air of the developed systems for April on daily basis data: (a) variation in humidity ratio and (b) variation in enthalpy

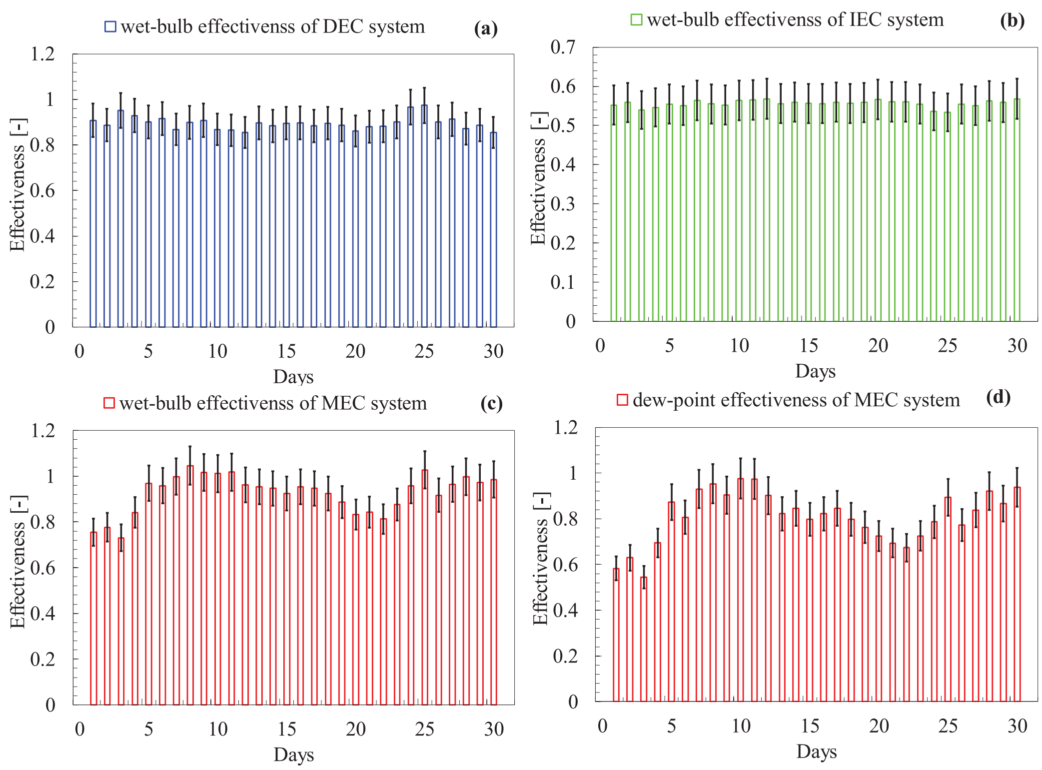

Fig. 11 Detailed description of the effectiveness (along with error bars) achieved by the developed systems using daily basis variation for April: (a) wet-bulb effectiveness of DEC system, (b) wet-bulb effectiveness of IEC system, (c) wet-bulb effectiveness of MEC system, and (d) dew-point effectiveness of MEC system

Figure 13 shows the operational cost comparisons between the develop EC systems and conventional VCAC system. The VCAC system consumes high primary energy than any of the developed EC system. Therefore, the study concluded that the developed EC systems are economical options to provide desired temperature and humidity to agricultural storage and livestock thermal comfort applications.

The required cooling loads for the optimum agricultural storage and livestock thermal comfort are estimated using the fundamental concepts presented in Section 3.2. In this regard, the ambient air conditions presented in Figure 6 are used. The cooling load changes with the change in ambient air conditions; therefore, performance of the developed EC systems varies temporally. The resulted cooling loads for the months of March to September are 4.25, 5.28, 6.02, 6.22, 5.85, 5.72, and 5.63 kW for agricultural products storage, and 32.0, 31.71, 31.51, 31.45, 31.55, 31.59, and 31.62 kW for livestock thermal comfort, respectively. For the rest of the months, there is no need of cooling for agricultural products

Table 4 The uncertainty analysis results of the effectiveness on monthly basis for the MEC, DEC, and IEC systems

Month	Uncertainty in wet-bulb effectiveness [—]		
	MEC	DEC	IEC
Jan	± 0.17	± 0.15	± 0.17
Feb	± 0.13	± 0.11	± 0.13
Mar	± 0.09	± 0.09	± 0.10
Apr	± 0.08	± 0.08	± 0.09
May	± 0.07	± 0.07	± 0.07
Jun	± 0.06	± 0.06	± 0.06
Jul	± 0.05	± 0.05	± 0.06
Aug	± 0.05	± 0.05	± 0.06
Sep	± 0.06	± 0.06	± 0.06
Oct	± 0.07	± 0.07	± 0.08
Nov	± 0.11	± 0.10	± 0.11
Dec	± 0.15	± 0.13	± 0.14
Average	± 0.09	± 0.08	± 0.09

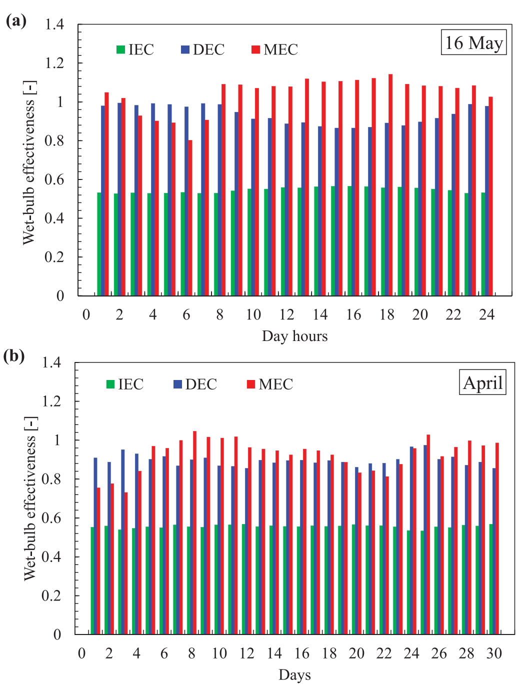

Fig. 12 Comparison of wet-bulb effectiveness of the developed EC systems: (a) hourly basis variation in effectiveness for 16-May, and (b) daily basis variation in effectiveness for April

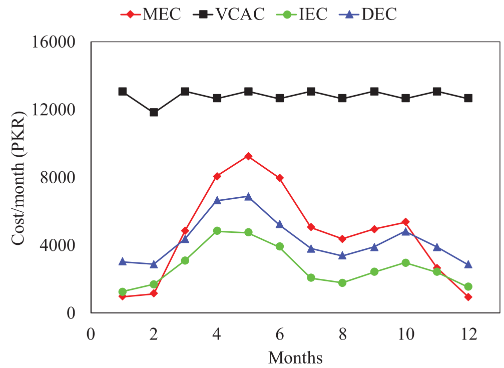

Fig. 13 Operational cost comparisons between develop EC systems and conventional 1-ton VCAC system

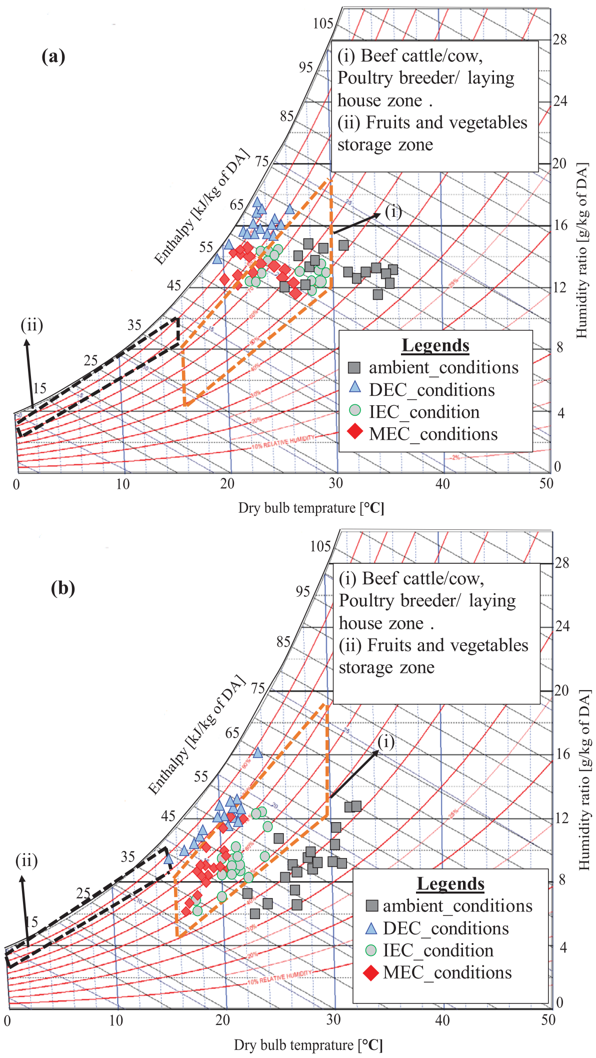

Fig. 14 Psychrometric representation of DEC, IEC and MEC systems: (a) for 16-May, and (b) for April

storage. Consequently, feasibility of the developed EC systems for agricultural product storage and livestock thermal comfort applications is determined. In this regard, ambient and product air conditions in terms of temperature and relative humidity are plotted on psychrometric charts as shown in Figure 14 for hourly (16-May) and daily basis (April) data. It can be seen that the developed EC systems are not feasible for the agricultural products storage at the hourly (Figure 14(a)) and the daily (Figure 14(b)) conditions. It is because the low temperature and high humidity (as presented in Figure 1) are required for the agricultural storage which were unable to be achieved by the developed EC systems. On the other hand, IEC and MEC systems achieved the required conditions for livestock thermal comfort application. Consequently, performance of the developed EC systems is analyzed for complete year using daily basis data. The whole year results are summarized in Table 5. The table clearly explains the feasibility situation of the developed EC systems for both applications. The IEC and MEC are feasible for livestock application from March to June. However, the DEC system is not feasible because it increases the moisture in air which disturbs the thermal comfort. Ambient air conditions of Multan are feasible from October to February (winter season) for many agricultural storage and livestock thermal comfort applications.

Table 5 Results of developed systems for agricultural product storage and livestock application for Multan (Pakistan)

	Agricultural product storage			Livestock application		
Month	DEC	IEC	MEC	DEC	IEC	MEC
Jan	N/A	N/A	N/A	N/A	N/A	N/A
Feb	N/A	N/A	N/A	N/A	N/A	N/A
Mar	x	x	x	N/A	o	o
Apr	x	x	x	x	o	o
May	x	x	x	x	o	o
Jun	x	x	x	x	o	o
Jul	x	x	x	x	x	x
Aug	x	x	x	x	x	x
Sep	x	x	x	x	N/A	N/A
Oct	N/A	N/A	N/A	N/A	N/A	N/A
Nov	N/A	N/A	N/A	N/A	N/A	N/A
Dec	N/A	N/A	N/A	N/A	N/A	N/A

Key: o: feasible, x: not-feasible, N/A: no need of EC systems.

5 Conclusions

The present study develops experimental apparatus for the performance evaluation of three kinds of evaporative cooling (EC) systems i.e. direct EC (DEC), indirect EC (IEC), and Maisotsenko cycle EC (MEC). The experimental data is obtained on hourly and daily basis for the climatic conditions of Multan (Pakistan). As expected, results indicate that the performance of EC systems is high at low relative humidity and high ambient air temperature. The experimental results displayed a noticeable cooling effect (i.e. difference of ambient and product air temperatures) which was ranging from 6.2 to 9.6 °C in the case of DEC system. On the basis of hourly data, the cooling effect was ranging from 3.2 to 6.2 °C and 5.3 to 12.3 °C for IEC and MEC systems, respectively. However, as per daily basis data, the cooling effect of DEC system was 8.5 °C, whereas, IEC and MEC systems were able to drop the temperature of ambient air to an average of 6.8 °C and 8.9 °C, respectively. The wet-bulb effectiveness of DEC, IEC, and MEC systems were ranging of 0.85–0.99, 0.55–0.56, and 0.85–0.98, respectively. According to the results, the developed EC systems consume relatively less energy as compared to conventional vapor compression systems which highlight the significance of EC systems. The cooling effect of DEC system could not provide desired conditions for agricultural storage and livestock thermal comfort applications in Multan conditions. On the other hand, IEC and MEC systems provided the required temperature and humidity conditions for livestock thermal comfort application from March to June, whereas, they were not feasible for many storage applications. Ambient air conditions of Multan are feasible from October to February for many agricultural storage and livestock thermal comfort applications.

Acknowledgements

This work is part of the PhD research of Mr. Hafiz Muhammad Umar Raza (1st Author). This research work has been carried out in the Department of Agricultural Engineering, Bahauddin Zakariya University, Multan, Pakistan. This research was funded by Bahauddin Zakariya University, Multan, Pakistan under the Director Research/ORIC grant entitled "Development and performance evaluation of prototypes of direct and indirect evaporative cooling-based air-conditioning systems", awarded to Principal Investigator Dr. Muhammad Sultan.

Electronic Supplementary Material (ESM): supplementary material is available in the online version of this article at https://doi.org/10.1007/s12273-020-0678-2.

References

Al Horr Y, Tashtoush B, Chilengwe N, Musthafa M (2020). Operational mode optimization of indirect evaporative cooling in hot climates. *Case Studies in Thermal Engineering*, 18: 100574.

Al-Zubaydi AYT, Hong G (2019). Experimental study of a novel water-spraying configuration in indirect evaporative cooling. *Applied Thermal Engineering*, 151: 283–293.

ASHRAE (2007). ASHRAE Handbook—HVAC applications. Atlanta, GA, USA: American Society of Heating, Refrigerating and Air-conditioning Engineers.

ASHRAE (2009). ASHRAE Handbook—Fundamentals. Atlanta, GA, USA: American Society of Heating, Refrigerating and Air-conditioning Engineers.

Amer O, Boukhanouf R, Ibrahim HG (2015). A review of evaporative cooling technologies. *International Journal of Environmental Science and Development*, 6: 111–117.

Ameur M, Kharbouch Y, Mimet A (2020). Optimization of passive design features for a naturally ventilated residential building according to the bioclimatic architecture concept and considering the northern Morocco climate. *Building Simulation*, 13: 677–689.

Arun BS, Mariappan V, Maisotsenko V (2020). Experimental study on combined low temperature regeneration of liquid desiccant and evaporative cooling by ultrasonic atomization. *International Journal of Refrigeration*, 112: 100–109.

Bruno F (2011). On-site experimental testing of a novel dew point evaporative cooler. *Energy and Buildings*, 43: 3475–3483.

Boonyasri M, Jamradloedluk J, Lertsatitthanakorn C, Therdyothin A, Soponronnarit S (2017). Increasing the efficiency of a thermoelectric generator using an evaporative cooling system. *Journal of Electronic Materials*, 46: 3043–3048.

Camargo JR, Ebinuma CD, Silveira JL (2005). Experimental performance of a direct evaporative cooler operating during summer in a Brazilian City. *International Journal of Refrigeration*, 28: 1124–1132.

Cihan E, Kavasoğulları B, Demir H (2020). Mass transfer correlation for tubular membrane-based liquid desiccant air-conditioning system. *Arabian Journal for Science and Engineering*, 45: 519–529.

Chen Z, Xu P, Feng F, Qiao Y, Luo W (2020). Data mining algorithm and framework for identifying HVAC control strategies in large commercial buildings. *Building Simulation*, https://doi.org/10.1007/s12273-019-0599-0

Dai YJ, Sumathy K (2002). Theoretical study on a cross-flow direct evaporative cooler using honeycomb paper as packing material. *Applied Thermal Engineering*, 22: 1417–1430.

Duan Z, Zhan C, Zhang X, Mustafa M, Zhao X, Alimohammadisagvand B, Hasan A (2012). Indirect evaporative cooling: Past, present and future potentials. *Renewable and Sustainable Energy Reviews*, 16: 6823–6850.

Dizaji HS, Hu EJ, Chen L, Pourhedayat S (2018). Development and validation of an analytical model for perforated (multi-stage) regenerative M-cycle air cooler. *Applied Energy*, 228: 2176–2194.

Doğramacı PA, Aydın D (2020). Comparative experimental investigation of novel organic materials for direct evaporative cooling applications in hot-dry climate. *Journal of Building Engineering*, 30: 101240.

Dong HW, Jeong JW (2020). Energy benefits of organic Rankine cycle in a liquid desiccant and evaporative cooling-assisted air conditioning system. *Renewable Energy*, 147: 2358–2373.

Jaafarian M (2018). An experimental investigation of the wind tower-assisted by the underground passive cooling system. *Building Simulation*, 11: 1179–1187.

Jeong SY, Tso CY, Zouagui M, Wong YM, Chao CYH (2018). A numerical study of daytime passive radiative coolers for space cooling in buildings. *Building Simulation*, 11: 1011–1028.

Karimi MT, Ghorbani GR, Kargar S, Drackley JK (2015). Late-gestation heat stress abatement on performance and behavior of Holstein dairy cows. *Journal of Dairy Science*, 98: 6865–6875.

Khalid O, Ali M, Sheikh NA, Ali HM, Shehryar M (2016). Experimental analysis of an improved Maisotsenko cycle design under low velocity conditions. *Applied Thermal Engineering*, 95: 288–295.

Laknizi A, Mahdaoui M, Ben Abdellah A, Anoune K, Bakhouya M, Ezbakhe H (2019). Performance analysis and optimal parameters of a direct evaporative pad cooling system under the climate conditions of Morocco. *Case Studies in Thermal Engineering*, 13: 100362.

Li Z, Lin B, Zheng S, Liu Y, Wang Z, Dai J (2020). A review of operational energy consumption calculation method for urban buildings. *Building Simulation*, 13: 739–751.

Lin J, Wang R, Li C, Wang S, Long J, Chua KJ (2020). Towards a thermodynamically favorable dew point evaporative cooler via optimization. *Energy Conversion and Management*, 203: 112224.

Mahmood MH, Sultan M, Miyazaki T, Koyama S, Maisotsenko VS (2016). Overview of the Maisotsenko cycle – A way towards dew point evaporative cooling. *Renewable and Sustainable Energy Reviews*, 66: 537–555.

Mahmood MH, Sultan M, Miyazaki T (2019). Significance of temperature and humidity control for agricultural products storage: overview of conventional and advanced options. *International Journal of Food Engineering*, 15(10): 20190063.

Mahmood MH, Sultan M, Miyazaki T (2020a). Experimental evaluation of desiccant dehumidification and air-conditioning system for energy-efficient storage of dried fruits. *Building Services Engineering Research and Technology*, 41: 454–465.

Mahmood MH, Sultan M, Miyazaki T (2020b). Solid desiccant dehumidification-based air-conditioning system for agricultural storage application: Theory and experiments. *Proceedings of the Institution of Mechanical Engineers, Part A: Journal of Power and Energy*, 234: 534–547.

Matsui K, Thu K, Miyazaki T (2020). A hybrid power cycle using an inverted Brayton cycle with an indirect evaporative device for waste-heat recovery. *Applied Thermal Engineering*, 170: 115029.

Miyazaki T, Akisawa A, Nikai I (2011). The cooling performance of a building integrated evaporative cooling system driven by solar energy. *Energy and Buildings*, 43: 2211–2218.

Mohapatra AK, Sanjay (2013). Analytical investigation of parameters affecting the performance of cooled gas turbine cycle with evaporative cooling of inlet air. *Arabian Journal for Science and Engineering*, 38: 1587–1597.

Mohapatra D, Mishra S, Giri S, Kar A (2013). Application of hurdles for extending the shelf life of fresh fruits. *Trends in Post-Harvest Technology*, 1(1): 37–54.

Niaz H, Sultan M, Khan AA, Miyazaki T, Feng Y, et al. (2019). Study on evaporative cooling assisted desiccant air-conditioning system for livestock application in Pakistan. *Fresenius Environmental Bulletin,* 28(11A): 8623–8633.

Nayak AK, Hagishima A, Tanimoto J (2020). A simplified numerical model for evaporative cooling by water spray over roof surfaces. *Applied Thermal Engineering*, 165: 114514.

Patel BB, Roy FS, Saiyad MJS, Joshi DC (2016). Respiration behaviour and heat of respiration of mango (cv. Langdo) under different storage conditions. *International Journal of Agriculture, Environment and Biotechnology*, 9: 855–859.

Rafique MM, Gandhidasan P, Rehman S, Al-Hadhrami LM (2015). A review on desiccant based evaporative cooling systems. *Renewable and Sustainable Energy Reviews*, 45: 145–159.

Ravindra MR, Goswami TK (2008). Modelling the respiration rate of green mature mango under aerobic conditions. *Biosystems Engineering*, 99: 239–248.

Raza SA, Khan AS, Malik A, Amin M, Asad H, Razzaq K (2013). Respiration rate, physico-chemical fruit quality and consumer acceptability for Fajri mango under different storage temperatures. *Pakistan Journal of Agricultural Sciences*, 50: 585–590.

Riangvilaikul B, Kumar S (2010). An experimental study of a novel dew point evaporative cooling system. *Energy and Buildings*, 42: 637–644.

Rose MT, Obara Y, Fuse H, Itoh F, Ozawa A, et al. (1996). Effect of growth hormone-releasing factor on the response to insulin of cows during early and late lactation. *Journal of Dairy Science*, 79: 1734–1745.

Senthilkumar K, Srinivasan PSS (2012). A parametric and experimental study of a centrifugal atomizer fitted in an industrial shed located in a tropical climate. *Arabian Journal for Science and Engineering*, 37: 1089–1100.

Sibanda S, Workneh TS (2020). Performance evaluation of an indirect air cooling system combined with evaporative cooling. *Heliyon*, 6: e03286.

Sghiouri H, Charai M, Mezrhab A, Karkri M (2020). Comparison of passive cooling techniques in reducing overheating of clay-straw building in semi-arid climate. *Building Simulation*, 13: 65–88.

Sultan M, Miyazaki T (2017). Energy-efficient air-conditioning systems for nonhuman applications. In: Ekren O (ed), Refrigeration. London: IntechOpen.

Sultan M, Miyazaki T, Mahmood MH, Khan ZM (2018). Solar assisted evaporative cooling based passive air-conditioning system for agricultural and livestock applications. *Journal of Engineering Science and Technology*, 13: 693–703.

Sultan M, Niaz H, Miyazaki T (2019). Investigation of desiccant and evaporative cooling systems for animal air-conditioning. In: Sultan M, Morosuk T (eds), Low-temperature Technologies, London: IntechOpen.

Stull R (2011). Wet-bulb temperature from relative humidity and air temperature. *Journal of Applied Meteorology and Climatology*, 50: 2267–2269.

Tariku F, Kumaran K, Fazio P (2011). Determination of indoor humidity profile using a whole-building hygrothermal model. *Building Simulation*, 4: 61–78.

Vakiloroaya V, Samali B, Fakhar A, Pishghadam K (2014). Thermo-economic optimization of rooftop unit's evaporator coil for energy efficiency and thermal comfort. *Building Simulation*, 7: 345–359.

Vala KV, Saiyed F, Joshi DC (2014). Evaporative cooled storage structures: An Indian Scenario. *Trends in Post Harvest Technology*, 2(3): 22–32.

Wan Y, Lin J, Chua KJ, Ren C (2018). Similarity analysis and comparative study on the performance of counter-flow dew point evaporative coolers with experimental validation. *Energy Conversion and Management*, 169: 97–110.

Wang X, Zhang G, Choi CY (2018). Effect of airflow speed and direction on convective heat transfer of standing and reclining cows. *Biosystems Engineering*, 167: 87–98.

Warke DA, Deshmukh SJ (2017). Experimental analysis of cellulose cooling pads used in evaporative coolers. *International Journal of Energy Science and Engineering*, 3(4): 37–43.

Xuan YM, Xiao F, Niu XF, Huang X, Wang SW (2012). Research and application of evaporative cooling in China: A review (I) – Research. *Renewable and Sustainable Energy Reviews*, 16: 3535–3546.

Yuan F, Chen Q (2012). Optimization criteria for the performance of heat and mass transfer in indirect evaporative cooling systems. *Chinese Science Bulletin*, 57: 687–693.

Yuan F, Dong W, Shen G, Li Y, Liu W (2020). Energy flow-based method for analysis and optimization of evaporative cooling and ventilation systems. *International Journal of Heat and Mass Transfer*, 146: 118865.

Zhan C, Duan Z, Zhao X, Smith S, Jin H, Riffat S (2011). Comparative study of the performance of the M-cycle counter-flow and cross-flow heat exchangers for indirect evaporative cooling—Paving the path toward sustainable cooling of buildings. *Energy*, 36: 6790–6805.

Zhang L, Zha X, Song X, Zhang X (2019). Optimization analysis of a hybrid fresh air handling system based on evaporative cooling and condensation dehumidification. *Energy Conversion and Management*, 180: 83–93.

Zhuang L, Chen X, Guan X (2020). A decentralized method for energy conservation of an HVAC system. *Building Simulation*, 13: 155–170.